

Channel-based Langevin approach for the stochastic Hodgkin-Huxley neuronYandong Huang,¹ Sten Rüdiger,² and Jianwei Shuai^{1,*}¹*Department of Physics and Institute of Theoretical Physics and Astrophysics, Xiamen University, Xiamen 361005, China*²*Institute of Physics, Humboldt-Universität zu Berlin, Berlin, Germany*

(Received 17 September 2012; revised manuscript received 7 December 2012; published 22 January 2013)

Stochasticity in ion channel gating is the major source of intrinsic neuronal noise, which can induce many important effects in neuronal dynamics. Several numerical implementations of the Langevin approach have been proposed to approximate the Markovian dynamics of the Hodgkin-Huxley neuronal model. In this work an improved channel-based Langevin approach is proposed by introducing a truncation procedure to limit the state fractions in the range of $[0, 1]$. The truncated fractions are put back into the state fractions in the next time step for channel noise calculation. Our simulations show that the bounded Langevin approaches combined with the restored process give better approximations to the statistics of action potentials with the Markovian method. As a result, in our approach the channel state fractions are disturbed by two terms of noise: an uncorrelated Gaussian noise and a time-correlated noise obtained from the truncated fractions. We suggest that the restoration of truncated fractions is a critical process for a bounded Langevin method.

DOI: [10.1103/PhysRevE.87.012716](https://doi.org/10.1103/PhysRevE.87.012716)

PACS number(s): 87.19.II, 87.10.Mn, 87.19.Hh

I. INTRODUCTION

Neuronal excitability and information transfer are determined by the currents through ion channels on the neuronal membrane. Hodgkin and Huxley first described the nerve membrane ion currents deterministically and established what is now called the Hodgkin-Huxley (HH) model [1]. The HH model is expressed by a set of differential equations to provide a deterministic description of the mean behavior of ion channel states. Later, from patch-clamp studies, the stochasticity of the opening and closing of ion channels, known as channel noise, has been observed [2].

With the stochastic HH model, many effects of channel noise on action potentials were studied, such as spontaneous action potentials [3,4], interspike interval statistics [5], stochastic resonance [6,7], and entropically enhanced excitability [8]. Beyond the basic HH model, the contribution of channel noise to neuronal dynamics has also been addressed with biophysically detailed model neurons, such as the entorhinal cortex neuron [9] and the cerebellar granule cell [10]. The critical roles of channel noise in the generation, propagation, and integration of neuronal signals have been investigated in a morphologically detailed neuronal model with extensive dendritic or axonal arborizations, such as in retinal ganglion cell [11], hippocampal neuron [12,13], and unmyelinated axon [14,15]. Besides intrinsic channel noise, external noise also exists in neural networks and is significant for neuronal activities [16]. The contribution of channel noise has become of interest also in many other systems or cells, such as intracellular calcium signaling system [17,18] and barnacle giant muscle fiber [19].

Besides the discussion of the effects of channel noise, a fundamental question is how to characterize the channel noise accurately. During the last 30 years, fractal ion-channel

behavior and history-dependent ionic current signals have been captured in experiment through analyzing the patch-clamp data [20–25]. Moreover, the analysis of the power spectra of nanochannel currents showed that such currents have the properties of the so-called $1/f$ (flicker) noise [26–28]. Actually, a biologically realistic neuronal system is complex with composite axon and dendritic structures, having a non-Markovian channel dynamics, and is affected by internal fluctuation of ion concentration and external noises. However, in this paper we focus only on the intrinsic Markovian noise described within a standard stochastic HH model.

By the HH model, all subunits in a channel are independent and each subunit has two discrete configuration states, i.e., the open and the closed states. Thus the channel dynamics can be simulated by a two-state Markovian process, which is termed the Markovian method [7,8,17,18,29,30]. In this paper the two-state Markovian method is considered as the standard method for comparison. For small channel numbers, a Markovian process can also be exactly simulated via a Gillespie-type algorithm [4,31–33]. However, these Markovian methods are computationally demanding in the case of many channels, leaving approximate methods more favorable [34].

Several approximate methods have been suggested to account for the Markovian channel noise. In the framework of Fox and Lu's work, two classes of approximations, termed subunit-based approaches and channel-based approaches, were proposed to represent the Markovian channel noise [17,35–37]. They are different essentially in the place where channel noise is added to the stochastic differential equations (SDEs). In detail, subunit-based Fox-Lu approaches add Gaussian noise to the equations that describe the fractions of subunit states of channels, while channel-based Fox-Lu approaches introduce Gaussian noise directly into the fractions of channel states. Subunit-based approaches are simpler and require less computational resources, which is why they have been applied extensively to stochastic neuron models [6], as well as calcium signaling models with stochastic IP3 receptors [17,18]. However, in comparison with the standard Markov method, subunit-based approaches could not capture correctly

*Corresponding author: Department of Physics, Xiamen University, Xiamen, Fujian 361005, China. FAX: (86) 592-218-9426. Email address: jianweishuai@xmu.edu.cn

the microscopic statistical properties of channel gating and the accuracy could not be improved with increasing numbers of channels [37–42].

On the other hand, the channel-based Fox-Lu approach was demonstrated to better replicate the statistical properties of the Markovian HH neuron [42]. However, there is an unreasonable treatment of channel state fractions in the channel-based Fox-Lu approach. Due to the addition of Gaussian noise to the SDEs, the fractions of channel states may be out of the range of $[0, 1]$, which will lack biological meaning. The original channel-based Fox-Lu approach does not consider confinement within $[0, 1]$ for the fractions of the eight states for Na^+ channels and five states for K^+ channels, but rather, the approach lets these fractions evolve freely without boundary limitation [42]. In the channel-based approach, two diffusion matrices have to be defined to calculate the state fractions for Na^+ and K^+ channels, respectively. The diffusion matrix has to be positive semidefinite in order to obtain real valued matrix square roots. Once a state fraction is out of $[0, 1]$, the diffusion matrices will no longer be guaranteed to be positive semidefinite. To avoid this problem, the equilibrium state fractions, rather than the real-time state fractions, of the channel are applied for the calculation of the diffusion matrices in the channel-based approach [42].

Another Langevin approach was developed recently based on the realization of an Ornstein-Uhlenbeck process [43]. However, this approach rests on the assumption that the channel number is large. At small channel number, this approach also generates negative open fractions for Na^+ and K^+ channels. Moreover, it has been found that this approach fails to track the Markov chain variance during the spikes even at large channel number [44]. More recently, a method with reflection was applied to the channel-based approach to make sure that the state fractions stay in the region of $[0, 1]$. However, it has also been pointed out that this reflected approach fails at small channel numbers [45]. In this paper we will show that the reflected approach could not give a satisfying estimate of the interspike interval even at large channel numbers.

Thus currently, although the Langevin approaches of the Markovian process are widely applied for the study of stochastic channel dynamics, none of them guarantees a precise description of channel noise in the neuronal system. In consequence, the use of the oversimplified channel noise in Langevin approaches may thereby lead to qualitatively correct but quantitatively incorrect conclusions. Thus, an important question is how to construct a better Langevin approach in order to correctly describe the Markovian channel dynamics.

In this paper we introduce an efficient Langevin method based on the channel-based Fox-Lu approach. In order to overcome the boundary-free problem, we consider a truncating method to hold the state fraction in the range of $[0, 1]$. Rather than simply cutting off the state fraction to $[0, 1]$, we feed the extra state fraction back into the system in the next time step for numerical calculation. Simulation results show that such a bounded channel-based approach can give a better approximation of the Markovian dynamics. Furthermore, we show that the restoring method, which is a key part in our bounded approach, can also be applied to the reflected Langevin approach to induce a better numerical result.

II. SIMULATION METHODS

In this section, we briefly review the HH model [1] and the corresponding Markov method. Then after introducing the original channel-based Langevin approach proposed by Fox and Lu [35,42] and the reflected SDEs approach proposed in [45], we present our improved bounded approach with the restoration process of truncated fractions. In the end, the restoration process is incorporated into the reflected SDEs approach.

A. HH model with subunit-based expression

We consider a single-compartment HH model [46], in which the neuronal membrane voltage evolution is governed by [1]

$$-C \frac{dV}{dt} = I_{\text{Na}} + I_{\text{K}} + I_L - I_{\text{stim}} \quad (1)$$

where V is the membrane potential in millivolts; $C = 1 \mu\text{F}/\text{cm}^2$ the membrane capacitance, and I_{stim} is the stimulus current added to the neuron in $\mu\text{A}/\text{cm}^2$. I_{Na} , I_{K} , and I_L are the currents of the sodium channels, potassium channels, and leakage channels, respectively, given by

$$I_{\text{Na}} = g_{\text{Na}} h m^3 (V - E_{\text{Na}}), \quad (2)$$

$$I_{\text{K}} = g_{\text{K}} n^4 (V - E_{\text{K}}), \quad (3)$$

$$I_L = g_L (V - E_L), \quad (4)$$

where $E_{\text{Na}} = 50 \text{ mV}$, $E_{\text{K}} = -77 \text{ mV}$, and $E_L = -54.3 \text{ mV}$ are the reversal potential of sodium channels, potassium channels, and leakage channels, respectively, and $g_{\text{Na}} = 120 \text{ ms}/\text{cm}^2$, $g_{\text{K}} = 36 \text{ ms}/\text{cm}^2$, and $g_L = 0.3 \text{ ms}/\text{cm}^2$ are the total conductance of sodium channels, potassium channels, and leakage channels, respectively.

The currents given by Eqs. (2) and (3) indicate that there are four identical and independent n subunits for each K^+ channel and three m subunits and one h subunit for each Na^+ channel. The original derivation of the HH equations was based on subunits, where the open probability $w = \{m, h, n\}$ of each subunit is described by the relaxation equations:

$$\frac{dw}{dt} = \alpha_w (1 - w) - \beta_w w. \quad (5)$$

Here α_w and β_w are subunit opening and closing rates with the unit of ms^{-1} and depend on the membrane potential V according to the following formulas:

$$\alpha_m = \frac{0.1(V + 40)}{1 - \exp[-(V + 40)/10]}, \quad (6)$$

$$\beta_m = 4 \exp[-(V + 65)/18], \quad (7)$$

$$\alpha_h = 0.07 \exp[-(V + 65)/20], \quad (8)$$

$$\beta_h = \frac{1}{1 + \exp[-(V + 35)/10]}, \quad (9)$$

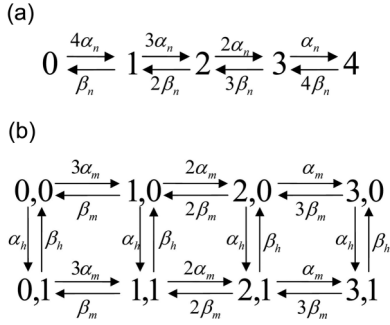


FIG. 1. Transition diagrams of channel states for K^+ (a) and Na^+ (b) channels. The code indicates how many subunits in the channel are in open state. In (a) code 4 represents four open n subunits for an open K^+ channel. In (b) code 3,1 represents three open m subunits and one open h subunit for an open Na^+ channel.

for m and h subunits of sodium channels, and

$$\alpha_n = \frac{0.01(V + 55)}{1 - \exp[-(V + 55)/10]}, \quad (10)$$

$$\beta_n = 0.125 \exp[-(V + 65)/80], \quad (11)$$

for n subunits of potassium channels.

B. HH model with channel-based expression

An equivalent expression of the deterministic subunit-based HH model is based on the dynamics of channel states. For the K^+ channel the four n subunits define a transition diagram of five channel states, as shown in Fig. 1(a). While for the Na^+ channel the three m subunits and one h subunit define a transition diagram of eight channel states, as given in Fig. 1(b). Denoting the channel state fractions x_i [$i = 0, 1, 2, 3, 4$ in Fig. 1(a)] for K^+ channels and y_{jk} [$j = 0, 1, 2, 3$ and $k = 0, 1$ in Fig. 1(b)] for Na^+ channels, we introduce two fraction vectors of channel state $\vec{X} = \{x_i\}$ and $\vec{Y} = \{y_{j+2k} \equiv y_{jk}\}$, respectively.

By considering the mass action kinetics with the transition diagram of channel states, the equations to describe the channel state fractions are written

$$\frac{d\vec{X}}{dt} = A_K \vec{X}, \quad (12)$$

$$\frac{d\vec{Y}}{dt} = A_{Na} \vec{Y}, \quad (13)$$

where A_K and A_{Na} are transition matrices of channel states, which can be found in Ref. [42].

Note that, among the 13 fractions of channel states, 11 states are independent due to the two constrains:

$$\sum_{i=0}^4 x_i = 1, \quad (14)$$

$$\sum_{j=0}^3 \sum_{k=0}^1 y_{jk} = 1. \quad (15)$$

Here fraction x_4 and y_{31} are the open probabilities of K^+ channels and Na^+ channels, respectively. Then the channel currents are given by $I_K = g_K x_4 (V - E_K)$ and $I_{Na} = g_{Na} y_{31} (V - E_{Na})$.

C. Markovian method of stochastic HH model

For the stochastic HH model, we directly simulate the stochastic dynamics for each single subunit by a two-state Markov process. In detail, all the subunits of the channels in the system are traced and updated for every small time step Δt . If a subunit is closed at time t , then the probability that it remains closed at time $t + \Delta t$ is $\exp(-\alpha \Delta t) \approx 1 - \alpha \Delta t$ with open rate α defined in Eqs. (6)–(11), giving an open probability $\alpha \Delta t$. If a subunit is open at time t , then the probability that it remains open at time $t + \Delta t$ is $\exp(-\beta \Delta t) \approx 1 - \beta \Delta t$ with closing rate β defined in Eqs. (6)–(11), giving a closing probability $\beta \Delta t$. Random numbers homogeneously distributed in $[0, 1]$ are generated at each time step and compared with these transition probabilities in order to determine the state of the channel subunit at each time step.

With the knowledge of open channel numbers N_{Na}^{Open} and N_K^{Open} among the total numbers N_{Na} and N_K for Na^+ and K^+ channels, respectively, the channel currents are then given by $I_{Na} = g_{Na} N_{Na}^{\text{Open}} / N_{Na} (V - E_{Na})$ and $I_K = g_K N_K^{\text{Open}} / N_K (V - E_K)$.

In the model, we keep the distribution densities of both the Na^+ and K^+ channels fixed with the density of the Na^+ channel three times as big as that of the K^+ channel [7]. By changing the membrane area, both the sodium and potassium channel numbers are changed.

Assuming all potassium channels identical and independent statistically, the distribution of the total open channel number at any given time will be a binomial distribution with population parameter N_K and bias parameter \bar{x}_4 . Then one can derive the analytical mean fraction $\langle P_K \rangle$ and the corresponding standard deviation DP_K of open K^+ channels [42]:

$$\langle P_K \rangle = \bar{x}_4, \quad DP_K = \sqrt{\langle P_K \rangle (1 - \langle P_K \rangle) / N_K}, \quad (16)$$

where $\langle \cdot \rangle$ denotes the average operation. Similar results can be obtained for the Na^+ channels.

D. Langevin model (A): Unbounded approach

The Langevin approach based on channel state expression of the HH model was introduced originally by Fox and Lu [35] and has been recently discussed in [42]. After considering the channel noise the channel state fractions are governed by the master equations, given as [35]

$$\frac{d\vec{X}}{dt} = A_K \vec{X} + S_K \vec{\xi}_K, \quad (17)$$

$$\frac{d\vec{Y}}{dt} = A_{Na} \vec{Y} + S_{Na} \vec{\xi}_{Na}, \quad (18)$$

where $\vec{\xi}_K$ and $\vec{\xi}_{Na}$ are noise vectors with each element an uncorrelated Gaussian white noise with zero mean and unit variance [47], and S_K and S_{Na} are the matrix square root of the diffusion matrices D_K and D_{Na} , respectively. The diffusion matrices D_K and D_{Na} can be found in Ref. [42].

In order to obtain real values of S_K and S_{Na} , the diffusion matrices should be positive semidefinite. Thus, instead of real-time values of x_i and y_{jk} which may be negative due to the Gaussian noise in Eqs. (12) and (13), the equilibrium fractions of x_i and y_{jk} are used in the diffusion matrices D_K and D_{Na} ,

given by

$$\bar{x}_i = \binom{4}{i} \frac{\alpha_n^i \beta_n^{4-i}}{(\alpha + \beta)^4}, \quad (19)$$

$$\bar{y}_{jk} = \binom{3}{j} \frac{\alpha_m^j \beta_m^{3-j} \alpha_h^k \beta_h^{1-k}}{(\alpha_m + \beta_m)^3 (\alpha_h + \beta_h)}. \quad (20)$$

For numerical simulation, Eq. (17) will be rewritten as the following difference iteration equation:

$$\bar{X}^{t+\Delta t} = \bar{X}^t + \Delta t A_K \bar{X}^t + \sqrt{\Delta t} S_K \bar{\xi}^t \quad (21)$$

In the simulation, each Gaussian noise is calculated by two white noises homogeneously distributed from 0 to 1. There is a similar difference equation for the fraction vector \bar{Y} in Eq. (18).

Numerically, although the normalization condition given by Eqs. (14) and (15) can be always satisfied with the difference equation Eq. (21), the large enough Gaussian noises may drive the state fractions x_i and y_{jk} out of range $[0, 1]$. Thus in the rest of this paper we call this original channel-based Langevin approach the unbounded method.

In the deterministic HH model, the open fractions x_4 and y_{31} of sodium and potassium channels change in the ranges of $[0, 0.35)$ and $[0, 0.25)$ during an action potential. With the unbounded Langevin approach we did not observe the situation of x_4 and y_{31} larger than 1; however, x_4 and y_{31} are frequently found to be negative. The probabilities for the open fractions x_4 and y_{31} to be negative are calculated, showing that even for a channel number as large as $N = 10000$, the open fraction y_{31} can become negative with a probability of 5%. At small channel number, the state fractions x_i and y_{jk} violate the physical constraint $[0, 1]$ seriously, which will cause the overflow and breakdown of the simulation program.

E. Langevin model (B): Reflected approach

The reflected approach was proposed in [45] to bound the solutions of the channel state fractions by incorporating the reflecting process with an orthogonal projection method (for more detail see [48]). Besides, an equivalent representation of the noise term is adopted so as to avoid the calculation of the square root of the diffusion matrix. The following is the corresponding formulations used in the numerical simulation of the reflected approach.

$$\bar{X}^{t+\Delta t} = \bar{X}^t + A_K \bar{X}^t \Delta t + \frac{1}{\sqrt{N_K}} L_K J_K \bar{\xi}_K \sqrt{\Delta t} + \Delta \bar{R}_K, \quad (22)$$

$$\bar{Y}^{t+\Delta t} = \bar{Y}^t + A_{Na} \bar{Y}^t \Delta t + \frac{1}{\sqrt{N_{Na}}} L_{Na} J_{Na} \bar{\xi}_{Na} \sqrt{\Delta t} + \Delta \bar{R}_{Na}, \quad (23)$$

where the matrices L_K , L_{Na} , J_K , J_{Na} as well as the definition of the reflecting processes \bar{R}_K and \bar{R}_{Na} can be obtained in Ref. [45].

F. Langevin model (C): Truncated and restored approach

Since the fractions of channel states should not be out of the range $[0, 1]$ we here introduce another scheme to confine the

state fractions x_i and y_{jk} within $[0, 1]$. In this method, we first cut off the state fractions that are out of the range $[0, 1]$. Before the cutting off, the state fractions obey the normalization condition. After cutting off, the normalization condition is broken. Thus a second step in our method is to consider a renormalization process for the state fractions. Thirdly, instead of simply throwing away the truncated values, we propose in our approach to store the truncated values for inclusion in the next time step.

Taking the K^+ channels as an example, we introduce a residue vector $\bar{E} = \{e_i\}$ in the numerical iteration function of Eq. (21),

$$\kappa_i^{t+\Delta t} = x_i^t + \sum_j A_{Kij} x_j^t \Delta t + \sum_j S_{Kij} \xi_j \sqrt{\Delta t} + e_i^t. \quad (24)$$

Compared to Eq. (21), a term e_i^t which is obtained from κ_i^t is added at the right-hand side of Eq. (24). Then we split $\kappa_i^{t+\Delta t}$ into the following two terms: $\kappa_i^{t+\Delta t} \equiv x_i^{t+\Delta t} + e_i^{t+\Delta t}$, where the residue vector $\bar{E} = \{e_i\}$ is the truncated value from the unbound vector $\bar{K} = \{\kappa_i\}$.

The truncation procedure is as follows: If all elements $\kappa_i^{t+\Delta t}$ in the unbounded vector $\bar{K} = \{\kappa_i\}$ are in the range of $[0, 1]$, then $x_i^{t+\Delta t} = \kappa_i^{t+\Delta t}$ and $e_i^{t+\Delta t} = 0$, and we go directly to the next iteration with Eq. (24). If any element $\kappa_i^{t+\Delta t}$ is out of the range of $[0, 1]$, we consider the following truncating procedure:

If there is an element $\kappa_i^{t+\Delta t} > 1$, then we define $x_i^{t+\Delta t} = 1$ and $e_i^{t+\Delta t} = \kappa_i^{t+\Delta t} - 1$. In order to preserve the normalization condition, we define $x_j^{t+\Delta t} = 0$ and $e_j^{t+\Delta t} = \kappa_j^{t+\Delta t}$ for other elements $j \neq i$.

Otherwise, if there is a term $\kappa_i^{t+\Delta t} < 0$, then we define $x_i^{t+\Delta t} = 0$ and $e_i^{t+\Delta t} = \kappa_i^{t+\Delta t}$. In order to preserve the normalization condition, we define $x_j^{t+\Delta t} = \kappa_j^{t+\Delta t} / \text{sum}$ and $e_j^{t+\Delta t} = \kappa_j^{t+\Delta t} - \kappa_j^{t+\Delta t} / \text{sum}$ with $\text{sum} = \sum_{j \neq i} \kappa_j^{t+\Delta t}$ for other elements $j \neq i$.

By this truncating procedure, the unbounded vector $\bar{K} = \{\kappa_i\}$ is split into two parts: the bounded vector \bar{X} and the residue vector \bar{E} . Then we put $\bar{X}^{t+\Delta t}$ into the iteration equation of Eq. (24) to calculate the state fractions at the next step. At the same time the residue vector $\bar{E}^{t+\Delta t}$ is restored to the fractions $\bar{X}^{t+\Delta t}$ by directly adding it to the right-hand side of Eq. (24) to obtain $\bar{K}^{t+2\Delta t}$.

As a result, the bounded approach defines the following two vector equations:

$$\begin{aligned} \bar{K}^{t+\Delta t} &= \bar{X}^t + A_K \bar{X}^t \Delta t + S_K \bar{\xi}_K \sqrt{\Delta t} + \bar{E}^t, \\ \bar{X}^{t+\Delta t} &= \bar{K}^{t+\Delta t} - \bar{E}^{t+\Delta t}. \end{aligned} \quad (25)$$

We repeat such truncating procedure at each time step with $e_i = 0$ at the beginning $t = 0$. Similar iteration equations can be written for Na^+ channels. With the above procedure, all the elements of vector \bar{X} and \bar{Y} are bounded within $[0, 1]$. Thus, instead of using the equilibrium state fractions given by Eqs. (19) and (20), the instantaneous state fractions x_i and y_{jk} are directly applied for the calculation of the diffusion matrices of D_K and D_{Na} in the bounded approach.

Obviously, since $\sum_{i=0}^4 x_i = 1$ is always maintained, we have $\sum_{i=0}^4 e_i = 0.0$. Putting two equations in Eq. (25) together,

we have the following equation:

$$\begin{aligned}\bar{X}^{t+\Delta t} &= \bar{X}^t + A_K \bar{X}^t \Delta t + (S_K \bar{\xi}_K^t - \bar{\eta}_K^t) \sqrt{\Delta t}, \\ \bar{\eta}_K^t &= (\bar{E}^{t+\Delta t} - \bar{E}^t) / \sqrt{\Delta t},\end{aligned}\quad (26)$$

where vector $\bar{\eta}_K^t = \{v_i^t\}$ with element v_i ($i = 0, 1, 2, 3, 4$). Similar as $\bar{\eta}_K = \{v_i\}$ for K^+ channels, vector $\bar{\eta}_{Na} = \{\omega_{jk}\}$ can also be defined for Na^+ channels. By comparing the difference iteration equations of Eqs. (21) and (26), one can see that the vectors $\bar{\eta}_K$ and $\bar{\eta}_{Na}$ in our Langevin approach can be considered as correlated or memory noise with zero mean, i.e., $\langle v_i^t \rangle = \langle \omega_{jk}^t \rangle = 0.0$.

G. Langevin model (D): Simple truncated approach

Alternatively, one may consider a simpler approach by applying Eq. (24) with the truncating and renormalizing procedures, but throwing away the residue vector \bar{E} , i.e.,

$$\begin{aligned}\bar{K}^t &= \bar{X}^t + A_K \bar{X}^t \Delta t + S_K \bar{\xi}_K^t \sqrt{\Delta t}, \\ \bar{X}^{t+\Delta t} &= \bar{K}^t - \bar{E}^{t+\Delta t}.\end{aligned}\quad (27)$$

However, our simulation results show that this approach could not reproduce the channel noise correctly for $N < 2000$ (data not shown). Thus in our paper we will not consider this approach.

H. Langevin model (E): Reflected and restored approach

The reflected approach applies the projection process to limit the fractions of channel states into the region of $[0, 1]$, and simply ignore the residue values which are also important in replicating correctly the stochastic channel dynamics. Here, we introduce the restoration operation into the original reflected approach. Taking Eq. (22) for the potassium channel as an example, the numerical iteration equation becomes

$$\bar{K}^{t+\Delta t} = \bar{X}^t + A_K \bar{X} \Delta t + \frac{1}{\sqrt{N_K}} L_K J_K \bar{\zeta}_K \sqrt{\Delta t} + \bar{E}^t \quad (28)$$

With the reflected procedure, we have $\bar{X}^{t+\Delta t} = \bar{K}^{t+\Delta t} + \Delta \bar{R}_K^{t+\Delta t}$. Here $\bar{X}^{t+\Delta t}$ is the channel state fraction after the reflected procedure. We then define the truncated fraction $\bar{E}^{t+\Delta t} = -\Delta \bar{R}_K^{t+\Delta t}$. This residue will be restored back in Eq. (28) for calculation in the next time step.

III. RESULTS

In this section, different Langevin approaches with diffusion matrices are discussed and compared with the two-state Markovian chain method (Markov). The original channel-based Fox-Lu approach will be called the unbounded approach (Unbound), the reflected Langevin approach suggested in Ref. [45] will be called the reflected approach (Reflected), the channel-based Langevin approach with truncated and restored state fractions is termed the truncated and restored approach (Truncated-Restored), and the reflected Langevin approach with restored state fractions is called the reflected and restored approach (Reflected-Restored). In all the following figures, we use a set of fixed symbols to represent the results obtained with the four methods. In detail, the black open squares are for the Markov method, the green plus symbols for the unbounded

approach, the purple cross symbols for the reflected approach, the red (gray) open squares for the reflected and restored approach, and the blue stars for the truncated and restored approach.

If not specified otherwise, we denote the K^+ channel number by N (i.e., $N \equiv N_K$) in the following, and the corresponding Na^+ channel number is then three times as large as N , (i.e. $N_{Na} = 3N$). Two typical stimulus currents are studied, i.e., $I_{stim} = 0$ and $15 \mu A/cm^2$, deterministically yielding a stable fixed point and a periodic oscillation, respectively.

A. Correlated noise for the truncated and restored approach

First, we discuss the equilibrium state which simulates the voltage-clamp experiments with a fixed membrane voltage V . Here we discuss the statistical properties of the memory noise defined in Eq. (26) for the truncated and restored approach and the memory noise for the reflected and restored approach.

As illustrated in Fig. 2(a), the standard deviations $\delta(v_4)$ and $\delta(\omega_{31})$ of memory noise v_4 and ω_{31} [see Eq. (26) for definition] decrease with increasing channel number. In Fig. 2(b) we discuss the characteristic times of autocorrelation functions for v_4 and ω_{31} , which are defined as

$$\tau_{v_4}(N) = \int_{\tau=0}^{\infty} \left| \frac{\langle v_4(N, t) v_4(N, t + \tau) \rangle}{\langle v_4(5, t) v_4(5, t) \rangle} \right| d\tau, \quad (29)$$

$$\tau_{\omega_{31}}(N) = \int_{\tau=0}^{\infty} \left| \frac{\langle \omega_{31}(N, t) \omega_{31}(N, t + \tau) \rangle}{\langle \omega_{31}(5, t) \omega_{31}(5, t) \rangle} \right| d\tau, \quad (30)$$

where $\langle \dots \rangle$ denotes the average over time t . Here the autocorrelation function is rescaled by the variance of memory noise at $N = 5$. One can see in Fig. 2(b) that a large characteristic time is found for the time series of v_4 and ω_{31} at a small channel number system, indicating a strong autocorrelation. Although

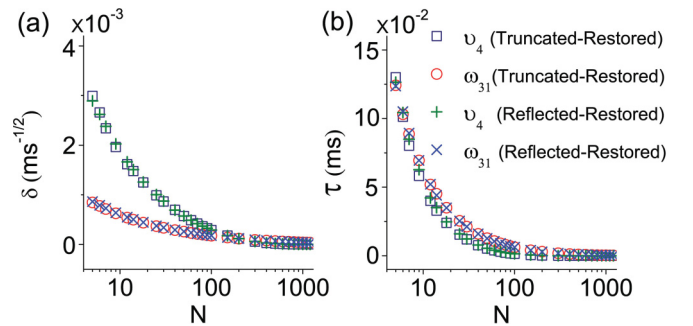


FIG. 2. (Color online) Statistical properties of memory noises defined in Eq. (26) at equilibrium states via channel number. (a) The standard deviation and (b) characteristic time of autocorrelation function of memory noises v_4 of K^+ channels and ω_{31} of Na^+ channels as a function of channel number N for the truncated and restored approach and the reflected and restored approach. In the simulation the stimulus $I_{stim} = 0 \mu A/cm^2$ and the voltage is fixed to $V = -65$ mV.

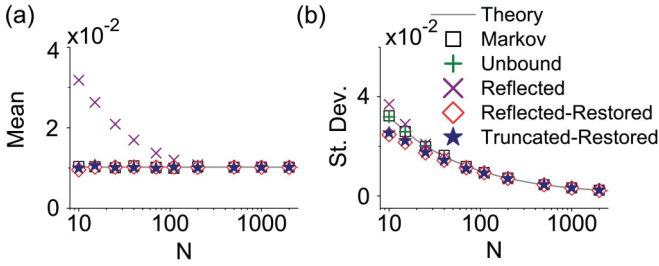


FIG. 3. (Color online) Statistical properties of the open fraction of K^+ channels at equilibrium states. The mean (a) and the standard deviation (b) of the open fractions of K^+ channel via the channel number at constant voltage $V = -65$ mV. In the simulation $I_{\text{stim}} = 0 \mu\text{A}/\text{cm}^2$.

the added Gaussian noises $\bar{\xi}_K$ and $\bar{\xi}_{Na}$ are time independent, the memory noises $\bar{\eta}_K$ or $\bar{\eta}_{Na}$ are autocorrelated.

B. Statistical properties of open fraction at constant voltage

Now we discuss the statistical properties of open fractions of channels at constant membrane voltage V . The mean and standard deviation of the open fraction can be analytically obtained by Eqs. (19) and (16) for K^+ channels, respectively. As shown in Fig. 3 by the analytical calculations (the gray lines) and the Markovian simulations, the mean of the fraction of open channels is independent of channel number [Fig. 3(a)], whereas the standard deviation inversely depends on N [Fig. 3(b)].

The numerical results with the four Langevin approaches are also given in Fig. 3. One can see that the unbounded approach generally gives a better approximation to the Markovian method than the three bound approaches. At large channel number all four approaches show satisfying agreement with the analytic results. The reflected approach exhibits the largest mean of the open fraction at small channel number.

C. The averaged maximal and minimal voltages via stimulus current

The channel noise generates the stochastic action potential with varying amplitude. The maximal and minimal membrane voltages are recorded during each time window of 0.1 s, during which several action potentials will typically be observed. Then the averaged maximal and minimal voltages can be calculated.

The averaged maximal and minimal voltages via constant stimulus current are plotted in Fig. 4 with different stochastic methods. Although all three Langevin approaches keep close agreement with the Markovian method at $N = 100$ [see Fig. 4(b)], the maximal voltages are evidently overestimated at $N = 10$ with the unbounded approach [Fig. 4(a)].

D. The moments of membrane voltage

Now we compare the moments of the membrane voltage with different Langevin approaches. In Fig. 5, the mean $\langle V \rangle$ and the standard deviation DV of membrane voltage are calculated as a function of N at $I_{\text{stim}} = 0.0$ and $15 \mu\text{A}/\text{cm}^2$.

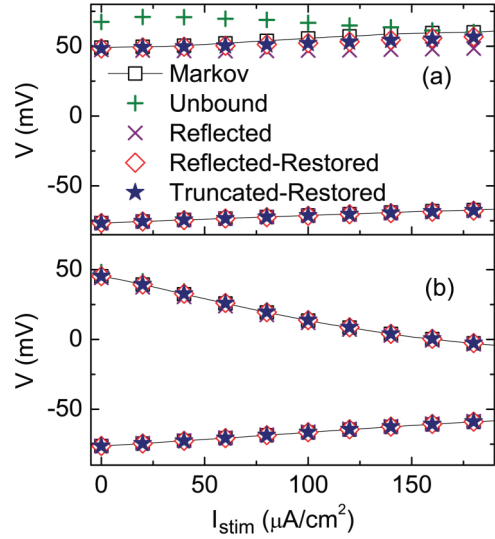


FIG. 4. (Color online) Bifurcation diagram of the membrane voltage as a function of stimulus current. The averaged maximal (upper symbols) and minimal voltages (lower symbols) as a function of stimulus current for stochastic neuron model at (a) $N = 10$ and (b) $N = 100$.

Our simulation shows that the unbounded approach can perform well on $\langle V \rangle$ and DV with large enough channel number at $N > 100$. In the range of $10 < N < 100$, the unbounded approach underestimates $\langle V \rangle$. The reflected approach gives a worse estimation of $\langle V \rangle$ at $N < 1000$. The failure of the reflected approach indicates that the truncated fractions play an important role in the channel dynamics. One can see that the truncated and restored approach and the reflected and restored approach both can give a reasonable estimation for the mean and the standard deviation of membrane voltage at $N > 50$.

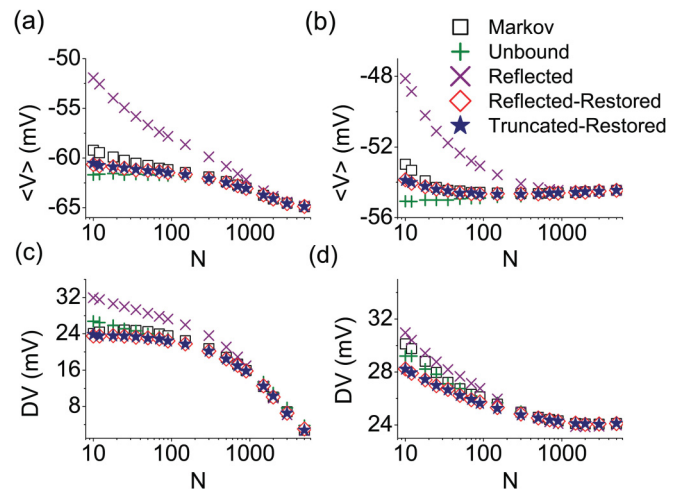


FIG. 5. (Color online) Statistical properties of membrane voltage. The mean (a), (b) and the standard deviation (c), (d) of the membrane voltage are plotted as a function of channel number N . Here $I_{\text{stim}} = 0.0 \mu\text{A}/\text{cm}^2$ is for the left column and $I_{\text{stim}} = 15.0 \mu\text{A}/\text{cm}^2$ for the right column.

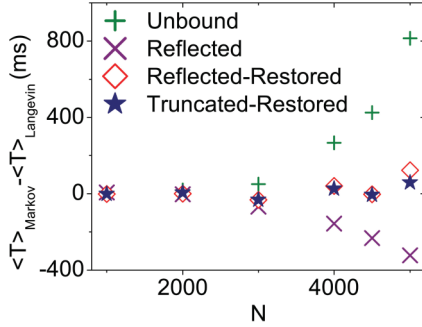


FIG. 6. (Color online) Comparison of the mean period of interspike intervals at large channel number. The difference of mean period of stochastic spikes obtained between the Markovian method and the Langevin approaches at large channel number ($N > 1000$). Here, $I_{\text{stim}} = 0.0 \mu\text{A}/\text{cm}^2$.

E. The interspike interval of stochastic action potentials

Next, we study the statistical properties of the stochastic action potentials. For neuronal functions, the important properties of the action potential are spike period, spike amplitude, and spike lifetime. In the deterministic HH neuron, once the voltage is beyond a critical threshold V_T , an action potential is triggered, giving a spike. For a stochastic channel dynamics, the membrane voltage shows a strongly fluctuating behavior, and a spike is defined as the action potential with voltage larger than the deterministic critical threshold V_T . The spike amplitude is defined as the difference in membrane potential from the peak voltage to the threshold. The stochastic channel dynamics can also cause the abortion of an action potential right after the voltage goes beyond the threshold. Thus, a fully developed spike is defined as having a minimal spike amplitude H_0 . In this paper, $H_0 = 30 \text{ mV}$ is considered. The spike lifetime is the duration measured at the half-of-spike amplitude. The interspike interval is defined as the time interval between two succeeding spike peaks.

The spike period $\langle T \rangle$ is the mean of the interspike intervals. In Fig. 6 we show the difference of mean period obtained for Markovian and Langevin approaches at large channel number ($N > 1000$) with $I_{\text{stim}} = 0.0 \mu\text{A}/\text{cm}^2$. It can be seen that the unbounded approach gives a shorter mean period of spontaneous action potential than the Markovian method, which has also been pointed out in Ref. [42]. These results indicate that the unbounded approach generates an unrealistically large channel noise to trigger spontaneous spikes at large N . Figure 6 also indicates that the reflected approach gives a longer mean period of spontaneous action potential compared to the Markovian method. However, the two Langevin approaches with restoration process can give a correct mean period at large channel number.

The spike period and its standard deviation DT obtained with the four methods are plotted in Fig. 7 at small channel number ($N < 1000$). Overall, the two Langevin approaches with restoration process show better approximation to those with the Markovian method. The reflected approach gives a short mean period of spikes at small channel number, indicating overestimation of the channel noise.

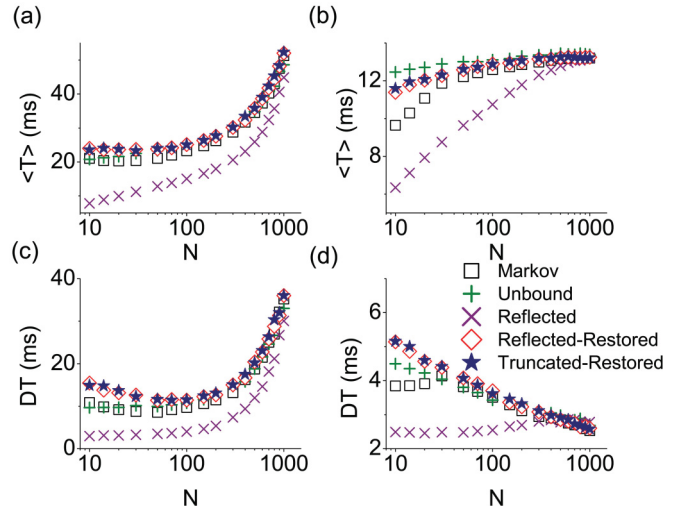


FIG. 7. (Color online) The mean period and standard deviation of the interspike intervals. The mean period $\langle T \rangle$ (a), (b) and standard deviation DT (c), (d) of interspike intervals via channel number N (< 1000). Here $I_{\text{stim}} = 0.0 \mu\text{A}/\text{cm}^2$ is for the left column and $I_{\text{stim}} = 15.0 \mu\text{A}/\text{cm}^2$ for the right column.

F. The amplitude of stochastic action potentials

The simulation results of mean amplitude $\langle H \rangle$ and its standard deviation DH are given in Fig. 8. The unbounded approach gives overestimated $\langle H \rangle$ for $N < 200$, while the reflected approach gives underestimated $\langle H \rangle$ for $N < 500$. However, the two Langevin approaches with restoration process show similar results for $\langle H \rangle$ and DH as those derived by the Markovian method.

G. The lifetime of stochastic action potentials

The simulation results of mean lifetime $\langle W \rangle$ of the spikes and its standard deviation DW are given in Fig. 9. It can be seen that all four Langevin approaches show similar results for

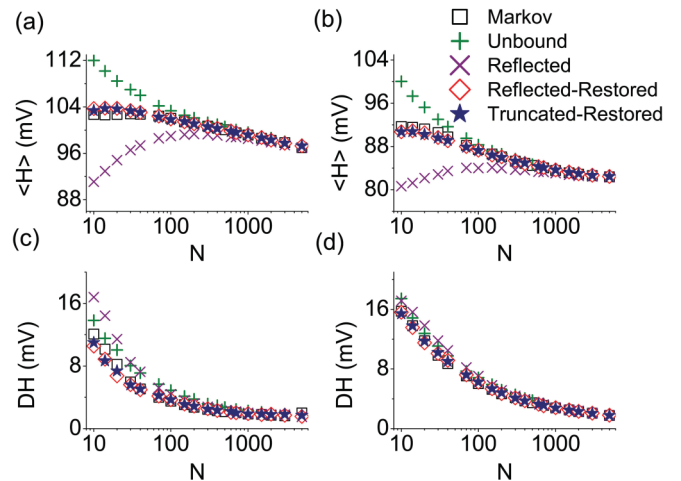


FIG. 8. (Color online) The mean amplitude and standard deviation of spike amplitude. The mean $\langle H \rangle$ (a), (b) and standard deviation DH (c), (d) of spike amplitude as a function of N . Here $I_{\text{stim}} = 0.0 \mu\text{A}/\text{cm}^2$ is for the left column and $I_{\text{stim}} = 15.0 \mu\text{A}/\text{cm}^2$ for the right column.

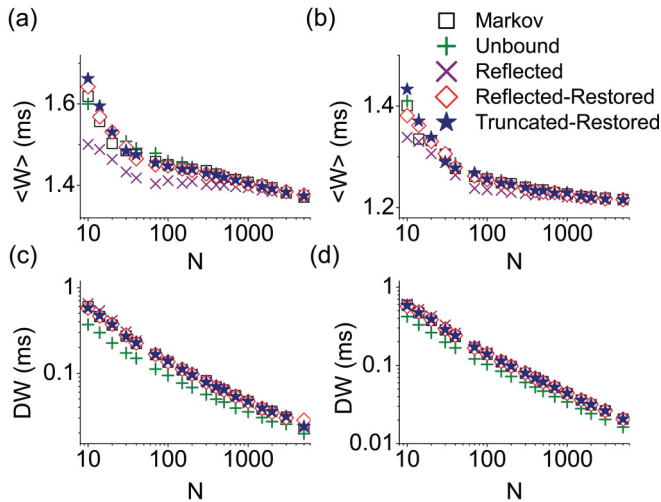


FIG. 9. (Color online) The mean lifetime and standard deviation of spike lifetime. The mean $\langle W \rangle$ (a), (b) and standard deviation DW (c), (d) of spike lifetime as a function of N . Here $I_{\text{stim}} = 0.0 \mu\text{A}/\text{cm}^2$ is for the left column and $I_{\text{stim}} = 15.0 \mu\text{A}/\text{cm}^2$ for the right column.

$\langle W \rangle$ as those derived by the Markovian method. However, the reflected approach underestimates $\langle W \rangle$ a little for $N < 200$.

IV. DISCUSSION

In this paper, we study improved computational approximations of noisy spike dynamics in the HH neuronal model. We use the Langevin approach with diffusion matrices, which was originally proposed by Fox and Lu to simulate the state fractions as continuous variables subjected to channel noise. Because of the Gaussian noise, the fractions of channel states in this approximation can in principle depart the interval $[0, 1]$. To amend this problem, we propose a bounded Langevin approach by introducing a truncation procedure to limit the state fractions in the range of $[0, 1]$ and then a renormalization procedure to satisfy the normalization condition for the state fractions. One unique process in our approach is that instead of simply neglecting the truncated values of state fraction, we feed the truncated fractions back into the state fractions during the next time step. The restoration procedure is also applied in the reflected Langevin approach [45].

Thus in this paper, the four Langevin approaches with diffusion matrices, including the original unbounded approach, the reflected Langevin approach [45], the truncated and restored approach, and the reflected and restored approach, are discussed and compared with the two-state Markovian chain method. By comparing the mean period of spikes and other parameters we show that for the original Langevin approach a satisfying approximation is obtained for potassium channel numbers in the range of 200–3000 and for the reflected Langevin approach in the range of 1000–3000, while for both the truncated and restored approach and the reflected and restored approach the numbers are in the range of > 50 .

For the neuron at equilibrium state with constant membrane voltage, we show that all four Langevin approaches can provide a satisfying approximation to the Markovian method. Especially, for the neuron at a dynamical situation, the two

bounded approaches with restoration process give a better approximation to the Markovian method than the unbounded approach.

The original unbounded Langevin approach proposed by Fox and Lu assumes that Markovian channel dynamics can be approximated by uncorrelated, zero-mean Gaussian noise. However, our simulation and previous studies clearly show that the simple consideration of Gaussian noise cannot adequately describe the Markovian channel dynamics, and the inaccuracy occurs even at large channel numbers. Thus, an important question is how to construct a correct noise term in the Langevin approach in order to appropriately describe the Markovian channel dynamics. Bruce suggests that a correlated and non-Gaussian noise with a nonzero mean should be considered [39].

In this paper, based on our bounded method, we give another answer to this question. On the one hand our method still applies the uncorrelated, zero-mean Gaussian noise to represent the channel noise. As a fact, in the HH neuron model the channel noise is basically a Markovian process, naturally calling for an uncorrelated Gaussian noise for Langevin approximation. On the other hand, with a Langevin approach such a Gaussian noise is considered to add upon the state fractions which have a limited range of $[0, 1]$. Driven by the Gaussian noise, the state fractions may be pushed out of that range. Thus we suggest that the question to construct a correct noise term in the Langevin approach then turns into the problem to construct a procedure to limit the unlimited state fractions.

In the original channel-based Langevin approach proposed by Fox and Lu, the state fractions just evolve freely, without any specific treatment on the extra value of state fractions. We think that such a free evolution of state fraction raises at least two issues: the frequently negative open fraction of K^+ channels at small channel number generates an unrealistic inward K^+ current, and the use of the equilibrium state fractions in the diffusion matrix could not correctly reflect the instantaneous strength of channel noise.

In our truncated and restored approach, we still assume that the Markovian channel dynamics can be simulated by uncorrelated Gaussian noise. Furthermore, the strength of the channel noise is determined by the instantaneous state fractions of channels. A unique process suggested in our approach is that we do not throw away the truncated extra values of state fractions. By putting the truncated fractions back into the state fractions in the next time step, we accurately preserve the strength of the Gaussian noise for channel stochasticity. Through the investigation of statistical properties of the membrane voltage, we show that the Langevin approaches with restoration procedure give a better agreement with the original dynamics.

The effectivity of the restoration process is also confirmed with the reflected Langevin approach [45]. For the reflected Langevin approach, a long mean period of spontaneous spikes is generated at large channel number, indicating that the channel noise is underestimated. While, at small channel number, a short mean period of spontaneous spikes is obtained, indicating that the channel noise is overestimated. However, our simulation shows that the reflected approach with restoration process can overcome these problems.

The procedure of truncation and restoration can be treated as a reorganization of the white Gaussian noise. As a result, the channel state fractions are disturbed by two sources of noise: an uncorrelated Gaussian noise and a time-correlated noise obtained from the truncation of unlimited state fractions.

The stochastic channel dynamics is found not only in neuron dynamics, but also in intracellular calcium signaling system [17,18] and muscle cells [19]. We suggest that the Langevin approach with the restoration of truncated state fractions can be applied to other Markovian channel systems. A similar procedure on state fractions may be considered to other Langevin approaches to avoid the state fraction out of range of [0, 1]. Our method is especially applicable to systems with large channel number. Recently, a binomial noise has been proposed to replace the Gaussian noise at small receptor number in nonlinear biochemical signaling [49]. It has been shown that the dynamics of most biologically realistic channels

are non-Markovian which should be produced with non-Gaussian noise. The two-state Markovian process, as well as the corresponding Langevin approaches with Gaussian noise, is a simple approximation. We believe that, with accurate representation of stochastic channel dynamics more quantitative insights on how channel noise modulates electrophysiological dynamics and function in cellular systems can emerge.

ACKNOWLEDGMENTS

J.S. acknowledges support from the National Natural Science Foundation of China under Grant No. 30970970 and the China National Funds for Distinguished Young Scientists under Grant No. 11125419. Computational support from the Key Laboratory for Chemical Biology of Fujian Province, Xiamen University, is gratefully acknowledged. S.R. acknowledges support from the Deutsche Forschungsgemeinschaft.

-
- [1] A. L. Hodgkin and A. F. Huxley, *J. Physiol.* **117**, 500 (1952).
 [2] B. Sakmann and E. Neher, *Single-Channel Recording*, 2nd ed. (Plenum Press, New York, 1995).
 [3] J. Clay and L. DeFelice, *Biophys. J.* **42**, 151 (1983).
 [4] C. Chow and J. White, *Biophys. J.* **71**, 3013 (1996).
 [5] P. Rowat, *Neural Comput.* **19**, 1215 (2007).
 [6] G. Schmid, I. Goychuk, and P. Hanggi, *Europhys. Lett.* **56**, 22 (2001).
 [7] P. Jung and J. W. Shuai, *Europhys. Lett.* **56**, 29 (2001).
 [8] J. W. Shuai and P. Jung, *Phys. Rev. Lett.* **95**, 114501 (2005).
 [9] J. A. White, R. Klink, A. Alonso, and A. R. Kay, *J. Neurophysiol.* **80**, 262 (1998).
 [10] A. Saarinen, M.-L. Linne, and O. Yli-Harja, *PLoS Comput. Biol.* **4**, e1000004 (2008).
 [11] M. C. W. van Rossum, B. J. O'Brien, and R. G. Smith, *J. Neurophysiol.* **89**, 2406 (2003).
 [12] K. Diba, H. A. Ester, and C. Koch, *J. Neurosci.* **24**, 9723 (2004).
 [13] R. C. Cannon, C. O'Donnell, and M. F. Nolan, *PLoS. Comput. Biol.* **6**, e1000886 (2010).
 [14] S. Zeng, Y. Tang, and P. Jung, *Phys. Rev. E* **76**, 011905 (2007).
 [15] A. A. Faisal and S. B. Laughlin, *PLoS Comput. Biol.* **3**, e79 (2007).
 [16] A. Carpio and I. Peral, *J. Nonlinear Sci.* **21**, 499 (2011).
 [17] J. W. Shuai and P. Jung, *Phys. Rev. Lett.* **88**, 68102 (2002).
 [18] P. Jung and J. W. Shuai, *Proc. Natl. Acad. Sci. USA* **100**, 506 (2003).
 [19] W. Gilles, T. Michele, and P. Khashayar, *Biol. Cybern.* **103**, 43 (2010).
 [20] L. S. Liebovitch and J. M. Sullivan, *Biophys. J.* **52**, 979 (1987).
 [21] S. J. Korn and R. Horn, *Biophys. J.* **54**, 871 (1988).
 [22] A. Fulinski, Z. Grzywna, I. Mellor, Z. Siwy, and P. N. R. Usherwood, *Phys. Rev. E* **58**, 919 (1998).
 [23] S. Mercik and K. Weron, *Phys. Rev. E* **60**, 7343 (1999).
 [24] S. B. Lowen, L. S. Liebovitch, and J. A. White, *Phys. Rev. E* **59**, 5970 (1999).
 [25] L. Liebovitch, D. Scheurle, M. Rusek, and M. Zochowski, *Methods* **24**, 359 (2001).
 [26] S. M. Bezrukov and M. Winterhalter, *Phys. Rev. Lett.* **85**, 202 (2000).
 [27] Z. Siwy and A. Fulinski, *Phys. Rev. Lett.* **89**, 158101 (2002).
 [28] I. D. Kosinska and A. Fulinski, *Europhys. Lett.* **81**, 50006 (2008).
 [29] J. W. Shuai, R. Sheng, and P. Jung, *Phys. Rev. E* **81**, 051913 (2010).
 [30] S. Rüdiger, J. W. Shuai, and I. M. Sokolov, *Phys. Rev. Lett.* **105**, 048103 (2010).
 [31] E. Skaugen and L. Walloe, *Acta Physiol. Scand.* **107**, 343 (1979).
 [32] D. T. Gillespie, *J. Phys. Chem.* **81**, 2340 (1977).
 [33] S. Rüdiger, J. W. Shuai, W. Huisinga, C. Nagaiah, G. Warnecke, I. Parker, and M. Falckey, *Biophys. J.* **93**, 1847 (2007).
 [34] H. Mino, J. T. Rubinstein, and J. A. White, *Ann. Biomed. Eng.* **30**, 578 (2002).
 [35] R. F. Fox and Y. N. Lu, *Phys. Rev. E* **49**, 3421 (1994).
 [36] R. F. Fox, *Biophys. J.* **72**, 2068 (1997).
 [37] Y. D. Huang, S. Rüdiger, and J. W. Shuai, *Eur. Phys. J. B* **83**, 401 (2011).
 [38] I. Bruce, *Ann. Biomed. Eng.* **35**, 315 (2006).
 [39] I. Bruce, *Ann. Biomed. Eng.* **37**, 824 (2009).
 [40] S. Zeng and P. Jung, *Phys. Rev. E* **70**, 011903 (2004).
 [41] B. Sengupta, S. B. Laughlin, and J. E. Niven, *Phys. Rev. E* **81**, 011918 (2010).
 [42] J. H. Goldwyn, N. S. Imennov, M. Famulare, and E. Shea-Brown, *Phys. Rev. E* **83**, 041908 (2011).
 [43] D. Linaro, M. Storace, and M. Giugliano, *PLoS Comput. Biol.* **7**, e1001102 (2011).
 [44] J. H. Goldwyn and E. Shea-Brown, *PLoS Comput. Biol.* **7**, e1002247 (2011).
 [45] C. E. Dangerfield, D. Kay, and K. Burrage, *Phys. Rev. E* **85**, 051907 (2012).
 [46] P. Dayan and L. Abbott, *Theoretical Neuroscience: Computational and Mathematical Modeling of Neural Systems* (MIT Press, Cambridge, MA, 2001).
 [47] A. Papoulis and S. U. Pillai, *Probability, Random Variables, and Stochastic Processes*, 4th ed. (McGraw-Hill Science/Engineering/Math, New York, 2002).
 [48] Y. Chen and X. Ye, [arXiv:1101.6081v2](https://arxiv.org/abs/1101.6081v2).
 [49] N. Bostani, D. A. Kessler, N. M. Shnerb, W. J. Rappel, and H. Levine, *Phys. Rev. E* **85**, 011901 (2012).